CrossMark

RESEARCH ARTICLE

Polybrominated diphenyl ethers (PBDEs) in background air around the Aegean: implications for phase partitioning and size distribution

Athanasios Besis[1] · Gerhard Lammel[2,3] · Petr Kukučka[2,4] · Constantini Samara[1] ·
Aysun Sofuoglu[5] · Yetkin Dumanoglu[6] · Kostas Eleftheriadis[7] · Giorgos Kouvarakis[8] ·
Sait C. Sofuoglu[5] · Vassiliki Vassilatou[7] · Dimitra Voutsa[1]

Abstract The occurrence and atmospheric behavior of tri- to deca-polybrominated diphenyl ethers (PBDEs) were investigated during a 2-week campaign concurrently conducted in July 2012 at four background sites around the Aegean Sea. The study focused on the gas/particle (G/P) partitioning at three sites (Ag. Paraskevi/central Greece/suburban, Finokalia/southern Greece/remote coastal, and Urla/Turkey/rural coastal) and on the size distribution at two sites (Neochorouda/northern Greece/rural inland and Finokalia/southern Greece/remote coastal). The lowest mean total (G + P) concentrations of $\sum_7$PBDE (BDE-28, BDE-47, BDE-66, BDE-99, BDE-100, BDE-153, BDE-154) and BDE-209 (0.81 and 0.95 pg m^{-3}, respectively) were found at the remote site Finokalia. Partitioning coefficients, K_P, were calculated, and their linear relationships with ambient temperature and the physicochemical properties of the analyzed PBDE congeners, i.e., the subcooled liquid pressure ($P_L°$) and the octanol-air partition coefficient (K_{OA}), were investigated. The equilibrium adsorption ($P_L°$-based) and absorption (K_{OA}-based) models, as well as a steady-state absorption model including an equilibrium and a non-equilibrium term, both being functions of log K_{OA}, were used to predict the fraction Φ of PBDEs associated with the particle phase. The steady-state model proved to be superior to predict G/P partitioning of BDE-209. The distribution of particle-bound PBDEs across size fractions < 0.95, 0.95–1.5, 1.5–3.0, 3.0–7.2, and > 7.2 μm indicated a positive correlation between the mass median aerodynamic diameter and log $P_L°$ for the less brominated congeners, whereas a negative correlation was observed for the high brominated congeners. The potential source regions of PBDEs were acknowledged as a combination of long-range transport with short-distance sources.

✉ Athanasios Besis
athanasb@chem.auth.gr

[1] Department of Chemistry, Environmental Pollution Control Laboratory, Aristotle University of Thessaloniki, Thessaloniki, Greece

[2] Research Centre for Toxic Compounds in the Environment, Masaryk University, Brno, Czech Republic

[3] Multiphase Chemistry Department, Max Planck Institute for Chemistry, Mainz, Germany

[4] School of Science and Technology, Man-Technology-Environment Research Center (MTM), Örebro University, Orebro, Sweden

[5] Department of Chemical Engineering and Environmental Research Center, Izmir Institute of Technology, Urla, Izmir, Turkey

[6] Department of Environmental Engineering, Dokuz Eylul University, Kaynaklar, Izmir, Turkey

[7] Institute of Nuclear Technology and Radiation Protection, NCSR Demokritos Institute, Athens, Greece

[8] Department of Chemistry, Environmental Chemical Processes Laboratory, University of Crete, Heraklion, Greece

Capsule abstract: Steady-state model appeared to better predict the observed Φ values for BDE-209 in comparison to the adsorption and the absorption models.

Introduction

Polybrominated diphenyl ethers (PBDEs) are additive brominated flame retardants (BFRs) that are added into plastics and foams without forming chemical bonds; therefore, their release from various consumer products in the environment is very likely (Besis and Samara 2012; Mandalakis et al. 2009).

As lipophilic compounds, PBDEs biomagnify in the food chain and bioaccumulate in living organisms (de Wit et al. 2010). Due to their similar structure to thyroid hormones (T3 and T4), they interfere with the body's hormone balance (endocrine disruptors; Shy et al. 2012). PBDEs can affect sexual development, the reproduction system, and the liver and kidney morphologies and cause developmental neurotoxicity (Chao et al. 2011). Therefore, the manufacture and usage of penta-, octa-, and deca-BDE, the three major commercial products in the global market mixtures (La Guardia et al. 2006), were prohibited in the European Union (Besis and Samara 2012) and voluntarily withdrawn in several US states, while in 2009, they were added to the list of persistent organic pollutants (POPs) under the Stockholm convention (UNEP/POPS/COP.4/17 2009).

PBDEs are semi-volatile organic compounds (SVOCs); therefore, in the environmentally relevant temperature range, they partition between the gas and particulate phases with the more volatile PBDEs found mostly in the former, while the higher molecular weight PBDEs found mostly in the latter (Besis et al. 2016; Cetin and Odabasi 2008; Chen et al. 2006; Cincinelli et al. 2014; He et al. 2014; Mandalakis et al. 2009; Yang et al. 2013). Gas–particle (G/P) partitioning along with degradation, deposition, and long-range atmospheric transport has a strong influence on the environmental fate of PBDEs (Xiao et al. 2012). Also, the particle-size distribution of PBDEs is a major factor determining their atmospheric behavior, thereby controling their removal mechanisms, the residence time and the transport potential (Besis et al. 2015). Studies regarding the particle-size distribution of PBDEs are relatively limited, indicating enrichment not only in the finest particle sizes (< 0.57 μm, Mandalakis et al. 2009; < 0.49 μm, Besis et al. 2015) but also in larger diameters (< 1.8 μm, Zhang et al. 2012).

Due to characteristic particle size and size selectivity of airways, humans are more exposed to the more toxic medium-brominated PBDEs (Shy et al. 2012). As Darnerud et al. (2001) reported of the three technical mixtures, penta-BDE seems to show chronic toxicological effects at the lowest concentration. Inhalation of PBDEs outdoors and indoors adds to the exposure of the population in the region (Ugranli et al. 2016) and should be quantified in comparison with other air pollutants.

The aim of the present study was to investigate the summertime atmospheric behavior of PBDEs at less polluted sites around the Aegean Sea, in the Eastern Mediterranean. Passive air sampling at ten sites in Greece and Turkey during summer 2012 revealed PBDE concentrations varying by more than one order of magnitude and dissimilar PBDE patterns across the countries (Lammel et al. 2015). In addition, previous studies in this area revealed higher particle-phase PBDEs levels in summer than in winter (Besis et al. 2015; Besis et al. 2016; Cetin and Odabasi 2008; Gevao et al. 2013). The reduced mixed layer and the weak west winds, characterizing the summer in Eastern Mediterranean, lead to reduced ventilation rates, preventing an effective dilution of the contaminants (Dayan et al. 2017). The present study presents the G/P partitioning of PBDEs, their mass size distribution, and explores the long-range transport potential during an intensive 2-week summertime sampling campaign concurrently carried out at four quasi-background sites around the Aegean Sea.

Materials and methods

Sample collection

The sampling campaign was concurrently carried out during July 2, 2012–July 13, 2012 at four sites: Neohorouda, northern Greece; Agia Paraskevi, central Greece; Finokalia, southern Greece; and Urla/Izmir, Turkey. A brief description of the site location and the meteorological conditions prevailing during the sampling campaign is provided in Table S1.

Gas- and particle-phase PBDEs were collected at Ag. Paraskevi, Finokalia, and Urla. A total of 23 day- and nighttime samples (air volume ≈ 100–150 m^3) were collected at Ag. Paraskevi using an Andersen high-volume active air sampler equipped with quartz fiber filters (QFFs) (10.2 cm diameter) and polyurethane foam (PUF) plugs (5.5 cm diameter, 7 cm thick). At Finokalia, two day- and nighttime samples (air volume ≈ 370 m^3) and ten 24-h samples (air volume ≈ 750 m^3) were collected using a high volume sampler with PM_{10} inlet (Digitel, Hegnau, Switzerland, flow rate 0.53 m^3 min^{-1}) equipped with QFFs (Whatman QMA 15 cm) and two PUF plugs (Gumotex Břeclav, density 0.030 g cm^{-3}, 11 cm diameter) in series. At Urla, a total of 22 day- and nighttime samples (air volume ≈ 197 and 134 m^3, respectively) were collected using a GPS-11 Thermo Andersen Inc. high volume sampler (flow rate 0.24 m^3 min^{-1}) equipped with GFFs (10.2 cm diameter) and two polyurethane foam (PUF) plugs plus one XAD2 resin trap sandwiched between them.

Size-resolved particulate PBDEs were collected at Neochorouda and Finokalia by impaction sampling. At Neohorouda, a high volume air sampler (Graseby-Andersen Ltd.) equipped with a four-stage inertial impactor (Sierra Instruments, model 234) with effective cutoff diameters 7.2, 3.0, 1.5, and 0.95 μm at the operational flow rate (1.1 m^3 min^{-1}) was used. At Finokalia, a high-volume sampler (HVS110, Baghirra, Prague, flow rate 1.1 m^3 min^{-1}) equipped with a six-stage cascade impactor (Andersen, PM_{10} inlet, cut-offs 7.2, 3.0, 1.5, 0.95, 0.49 μm) was employed. QFFs were

used as impaction substrates (slotted sheets 5.7 × 5.7 cm for the five coarser size fractions and rectangular backup sheets for the finest size fraction).

Analysis of PBDEs

Samples collected in each country were analyzed for PBDEs according to previously reported methods (Besis et al. 2015; Cetin and Odabasi 2007a; Cetin and Odabasi 2008; Cetin and Odabasi 2011; Lammel et al. 2015; Sofuoglu et al. 2013). The analytical methods applied by the participants differed with regard to sample, extraction, cleanup, and type of calibration procedures as well as regarding the analytical methods used for identification and quantification of PBDE congeners. Detailed information about the analytical procedures are provided in the Supplementary Material (S1) and summarized in Table S2.

Samples from Ag. Paraskevi and Finokalia were analyzed at the RECETOX, Brno, as described in Lammel et al. (2015). Briefly, PUFs and QFFs were spiked with surrogate standards and extracted using automated Soxhlet extraction with dichloromethane (DCM). HRGC/HRMS analysis was performed on a 7890A GC (Agilent, USA) coupled to AutoSpec Premier MS (Waters, Micromass, UK) using a 15 m × 0.25 mm × 0.10 μm RTX-1614 column (Restek, USA) (Table S2).

Samples from Urla were analyzed in the Izmir Institute of Technology (IzTech) and Dokuz Eylul University. Briefly, after spiking of surrogate standards, PUFs were Soxhlet extracted with acetone/hexane (1:1 v/v), while QFFs were extracted ultrasonically. PBDEs were analyzed in an Agilent 6890N gas chromatograph equipped with a DB5-MS (15 m × 0.25 mm × 0.1 μm) capillary column and coupled with a mass selective detector (Agilent 5973 inert MSD) working at electron capture negative chemical ionization (ECNI) mode (Table S2).

Samples from Neochorouda were analyzed in the Aristotle University of Thessaloniki (AUTh) according to Besis et al. (2015). Briefly, QFFs were spiked with surrogate standards and extracted with DCM/hexane (1:1 v/v) in a microwave extraction unit. PBDEs were analyzed in an Agilent 6890N gas chromatograph interfaced with an Agilent 5973 mass spectrometer working at electron impact ionization (EI) mode using a DB5-MS capillary column (15 m × 0.25 mm × 0.1 μm) (Table S2).

QA/QC

Sampling substrates were identically treated by all laboratories. Briefly, QFFs were baked out at 450 °C for 8 h prior to use to remove any organic contaminant and stored in aluminum foil packages. PUF plugs were Soxhlet-extracted for 8 h using acetone and for another 8 h using toluene. After drying, they were placed in solvent-rinsed glass jars with aluminum foil-lined lids. Loaded PUFs and QFFs were separately wrapped in two layers of aluminum foil and transported to the laboratory in cooling boxes. Upon receipt, they were put in zip-lock PE bags and kept refrigerated (− 18 °C) until analysis (max 3 months). To prevent any possible photolysis of PBDE analytes, special care was taken to avoid the exposure of samples to light during their storage and analysis.

Field blanks were used for all types of collected samples (QFFs, PUF plugs, and cascade impactor QFF substrates), and their values were subtracted from those of real samples. The concentrations of PBDEs congeners in field blanks were less than 10% of the concentration found in field samples. The levels of individual BDE congeners (mainly BDE-47, BDE-99, and BDE-209) in blank samples were very low, in most cases lower than the instrument detection limit (iLOD).

Recoveries of surrogate standards exhibited little variability between laboratories. The average recoveries for ^{13}C-BDE-15, BDE-28, BDE-47, BDE-99, BDE-153, BDE-154, BDE-183, BDE-204, BDE-207, and BDE-209 were 72 ± 11, 95 ± 8, 104 ± 8, 109 ± 7, 93 ± 8, 84 ± 7, 101 ± 10, 94 ± 15, 77 ± 14, and 79 ± 16, respectively. Recoveries of the target congeners ranged from 70 to 109%. Results were recovery corrected.

The limit of quantification (LOQ) of target compounds was calculated as three times the instrument limit of detection (iLOD), which in turn was based on the mean of three blanks plus three times the standard deviation. The LOQs ranged from 0.1 to 18 pg for individual PBDE congeners.

For QC/QA, the variability between laboratories was estimated. For this purpose, equal pieces from filters spiked with standard solution of PBDEs were analyzed in each laboratory. The results showed an acceptable variability between laboratories ranging from 30 to 45% for the dominant congeners.

Statistical analysis

All descriptive statistics were computed using SPSS version 20.0 (IBM company, Chicago, IL, USA) and Microsoft Excel 2007. The nonparametric Mann–Whitney U test and Spearman correlation coefficients were employed to evaluate the seasonal variability of PBDE levels and the relationships with meteorological conditions. Concentration values below LOD were treated as LOD/2 during all statistical analyses, and $p < 0.05$ was considered statistically significant.

Calculations of G/P partition parameters

Experimental G/P partitioning coefficients, K_P (m³ μg^{-1}), were calculated for all PBDE congeners that were found at quantifiable concentrations in both phases according to Eq. (1):

$$K_P = (C_p/TSP)/C_g \qquad (1)$$

where C_p and C_g are the analyte concentrations in particle (QFF) and gas (PUF) phases, respectively (both in pg m^{-3}), and TSP is the concentration of total suspended particles in air (μg m^{-3}).

The linear relationships between K_P and the subcooled liquid pressure ($P_L°$) of the compounds (Finizio et al. 1997; Harner and Bidleman 1998; Pankow 1998) were investigated using Eq. (2):

$$\log K_P = m \log P_L^{\,\circ} + b \qquad (2)$$

Temperature-corrected $P_L°$ values (Pa) were calculated from Eq. (3) (Tittlemier et al. 2002; Xu et al. 2007):

$$\log P_L^{\,\circ} = B/T + A \qquad (3)$$

using the average ambient temperature T during each sampling event, and the values suggested by Tittlemier et al. (2002) for parameters A and B.

The linear relationships between K_P and the octanol-air partition coefficient K_{OA} (Harner and Bidleman 1998; Pankow 1987) were investigated using Eq. (4):

$$\log K_P = m \log K_{OA} + b \qquad (4)$$

Temperature-corrected K_{OA} values were calculated from Eq. (5) (Harner and Shoeib 2002; Wang et al. 2008; Wania and Dugani 2003; Xu et al. 2007):

$$\log K_{OA} = A + B/T \qquad (5)$$

using the average ambient temperature during each sampling event, and the values suggested by Harner and Shoeib (2002) and Li et al. (2017) for parameters A and B.

K_P values predicted by the absorption model as a function of K_{OA} and the content of organic matter in particles (f_{om}) were calculated according to Eq. (6), assuming that all of the particulate organic matter is available for absorption of gaseous organic compounds (Harner and Bidleman 1998):

$$\log K_P = \log K_{OA} + \log f_{om} - 11.91 \qquad (6)$$

The average f_{om} content at Finokalia, calculated from the organic carbon content (OC) of particles by multiplying OC by a factor of 2.1, was 23% (Table S3). In lack of OC data, three f_{om} levels were considered for Urla (10, 20, and 55%).

In addition, the steady-state model recently suggested by Li et al. (2015) was considered using Eq. (7):

$$\log K_{Ps} = \log K_P + \log \alpha \qquad (7)$$

where K_{Ps} is the partition coefficient at steady-state conditions, $\log K_P$ is designated the equilibrium term, given by Eq. (6), and $\log \alpha$ is the non-equilibrium term caused by dry and wet deposition of particles (Li et al. 2015). The non-equilibrium term α is a function of f_{om} and K_{OA} according to Eq. (8):

$$\log \alpha = -\log(1 + G/C) \qquad (8)$$

where $C = 5$ and $G = 2.09 \times 10^{-10} f_{om} K_{OA}$ (Li et al. 2015).

The $P_L°$-based (Junge–Pankow, J–P) adsorption model, the K_{OA}-based absorption model, and the steady-state model were further used to predict the fraction Φ of PBDEs associated with the particle phase.

The particle mass fraction Φ in the $P_L°$-based (J–P) adsorption model was calculated from Eq. (9):

$$\Phi = c_J \theta / (P_L^{\,\circ} + c_J \theta) \qquad (9)$$

where c_J is a constant, related to the heat of condensation of the chemical and the surface properties, and θ is the aerosol surface density (Pankow 1987). The values used for c_J in the present study were 17.2 and 13.3 Pa cm (Cetin and Odabasi 2008; Chen et al. 2006; Pankow 1987). For particles in the size range 0.008–32 μm, θ was found to be $7.7 \pm 1.5 \times 10^{-5}$ cm^2 cm^{-3} at Finokalia. In lack of data, the same value was applied for samples collected at Urla.

In the absorption model, Φ was inferred from K_P using Eq. (10):

$$\Phi = \frac{K_P \text{TSP}}{1 + K_P \text{TSP}} \qquad (10)$$

The mean TSP concentrations at Finokalia and Urla were 28 and 36 μg m^{-3}, respectively (Table S3). In the steady-state model, Φ was also calculated from Eq. (10) considering K_{Ps} instead of K_P.

Results and discussion

Gas- and particle-phase concentrations of PBDEs

Mean gas- and particle-phase concentrations of the PBDE congeners (BDE-28, BDE-47, BDE-66, BDE-99, BDE-100, BDE-153, BDE-154, and BDE-209), which were commonly found at all sampling sites (excepting BDE-66 that was not detected at Urla) and the frequency of detection (%), are provided in Table 1 and Fig. 1. Comparative data for the total (G + P) PBDE levels reported in literature for various sites worldwide are provided in Table S4. In general, excluding BDE-209, the sum concentrations of the seven PBDE congeners (BDE-28, BDE-47, BDE-66, BDE-99, BDE-100, BDE-153, BDE-154) ($\sum_7$PBDE) in this study are within the range of corresponding values previously found at sites around the Aegean sea (5–55 pg m^{-3} of $\sum_5$PBDE in Izmir, Cetin and Odabasi 2008; 22 and 13 pg m^{-3} of $\sum_{12}$PBDE in Athens and Heraklion, Mandalakis et al. 2009; 9.4 pg m^{-3} of Σ_{12}PBDE in Thessaloniki, Besis et al. 2016) or the levels of $\sum_5$PBDE measured following passive sampling at rural and coastal sites around the Aegean sea (0.40 and 13.8 pg m^{-3}, Lammel et al. 2015). Also, the $\sum_7$PBDE concentrations found in this study are comparable to the $\sum_{14}$PBDE levels (excluding BDE-209) found at semi-urban (3–30 pg m^{-3}, Harner et al. 2006) and

Table 1 Average PBDE concentrations and frequency of detection in the gas and particle phases (pg m^{-3})

Compounds	Gas phase	F%	Particle phase	F%	Total (G + P)
Ag. Paraskevi (n = 23)					
BDE-28	1.32	100	0.002	17	1.32
BDE-47	12.3	100	< LOQ	0	12.3
BDE-66	0.219	98	< LOQ	0	0.219
BDE-100	0.902	100	< LOQ	0	0.902
BDE-99	3.69	100	< LOQ	0	3.69
BDE-154	0.209	100	< LOQ	0	0.209
BDE-153	0.144	91	< LOQ	0	0.144
$\sum_7$PBDE	18.8		0.002		18.8
BDE-209	7.87	52	8.22	4	16.1
Finokalia (n = 12)					
BDE-28	0.037	100	0.006	8	0.043
BDE-47	0.415	100	0.013	100	0.428
BDE-66	0.022	100	< LOQ	0	0.022
BDE-100	0.062	100	0.001	100	0.063
BDE-99	0.187	100	0.012	100	0.199
BDE-154	0.009	100	0.028	39	0.038
BDE-153	0.012	54	0.002	9	0.014
$\sum_7$PBDE	0.744		0.063		0.807
BDE-209	0.449	100	0.500	54	0.949
Urla (n = 22)					
BDE-28	0.816	91	0.635	100	1.45
BDE-47	4.93	36	0.822	36	5.75
BDE-66	NA		NA		NA
BDE-100	0.848	100	0.422	100	1.27
BDE-99	3.00	100	0.967	73	3.92
BDE-154	0.593	100	0.345	100	0.939
BDE-153	0.568	100	0.375	77	0.943
$\sum_7$PBDE	10.8		3.57		14.37
BDE-209	90	91	93	82	183

F% percentage of samples with concentration > LOQ, *NA* not analyzed

remote sites in Canada (1.2–55 pg m^{-3}, Xiao et al. 2012). By contrast, the levels of BDE-209 at Urla are similar to those found in and around Aliaga Industrial Area (AIA) (50 km north-northeast of the sampling site) and lower than those measured near ferrous scrap processing steel plants with electric arc furnaces in AIA (up to 3968 pg m^{-3} with an average of 1451 pg m^{-3}) and higher than those measured in Izmir located about 50 km east of the sampling site (Cetin and Odabasi 2008; Odabasi et al. 2009; Odabasi et al. 2015a; Odabasi et al. 2015b).

At all sites, $\sum_7$PBDE was significantly higher in the gas than in the particle phase accounting for almost 100, 92, and 75% of the total at Ag. Paraskevi, Finokalia, and Urla, respectively (Fig. 1). A 90% occurrence of PBDEs in the gas phase has also been found by ship measurements in central and eastern

Mediterranean during August–September 2010 (Mulder et al. 2015). The gas phase of individual PBDE congeners ranged between 55 and 100% of the total excepting BDE-154 at Finokalia that exhibited a lower gas-phase (25%) (Fig. 1). For BDE-209, equal partitioning between the two phases was observed at all sites. The prevalence of gas-phase PBDEs suggests that the three sampling sites are less impacted by anthropogenic point sources. Higher gas- than particle-phase concentrations have also been found at a semi-urban site in Heraklion, Crete (13 vs. 2 pg m^{-3} for $\sum_{12}$PBDE, Mandalakis et al. 2009), at an urban-background site in Thessaloniki (6.3 pg m^{-3} vs. 3.1 pg m^{-3} for $\sum_{12}$PBDE, Besis et al. 2016), as well as at rural and urban sites in Kuwait (26 vs. 7 and 52 vs. 7 pg m^{-3}, respectively for $\sum_7$PBDE, Gevao et al. 2013). By contrast, particle-phase exceeded the gas-phase concentration in the center of Athens (19 vs. 7 pg m^{-3} for $\sum_{12}$PBDE, Mandalakis et al. 2009) at a heavy-traffic site and at a industrial site in Thessaloniki (17.5 vs.11.1 and 23.7 vs. 21.1 pg m^{-3} for $\sum_{12}$PBDE, Besis et al. 2016), as well as at urban and industrial sites in Izmir, Turkey (Cetin and Odabasi 2008).

In agreement with other studies reporting higher concentrations of PBDEs at urban locations (Besis et al. 2016; Wang et al. 2012), the total (G + P) concentrations of $\sum_7$PBDE at Ag. Paraskevi and Urla (18.8 and 14.3 pg m^{-3}, respectively) were significantly higher ($p < 0.05$) than those determined at Finokalia (0.809 pg m^{-3}) highlighting the remote character of the latter site. PBDE levels at Finokalia, in particular, were lower than those found by ship measurements in central and eastern Mediterranean (4.3 pg m^{-3}) with air masses mostly originating from central Europe and partly crossing western Europe (Mulder et al. 2015). Finokalia also exhibited the lowest BDE-209 levels (0.949 pg m^{-3}) among all sites, while particularly high concentrations were found at Urla (more than ten times higher than those found at Ag. Paraskevi).

Mean total $\sum_7$PBDE concentrations were higher during daytime than nighttime at both Ag. Paraskevi and Urla (25.9 vs. 11.6 and 11.3 vs. 10.5 pg m^{-3}, respectively); although statistically, a significant difference was found only at Ag. Paraskevi ($p < 0.05$). The higher daytime $\sum_7$PBDE levels are probably related to the higher temperatures occurring during the day (Fig. 2). However, transport from the center of Athens and/or the heavily industrialized Thriassion Plain located 10–35 km southwest of Ag. Paraskevi as a result of the sea breeze circulation during daytime is a more plausible explanation. By contrast, BDE-209 showed slightly higher total levels during nighttime (9.2 vs.7.3 pg m^{-3} at Ag. Paraskevi; 184 vs. 179 pg m^{-3} at Urla) (Fig. 2), but the differences were not statistically significant ($p > 0.05$). The higher nighttime concentrations of BDE-209 may be due to its photodegradation during daytime (Besis and Samara 2012). In adition in all sampling sites, microclimatic conditions during nighttime (i.e., lower wind speed and mixing height) are expected to cause increased PBDE concentrations due to poor dispersion.
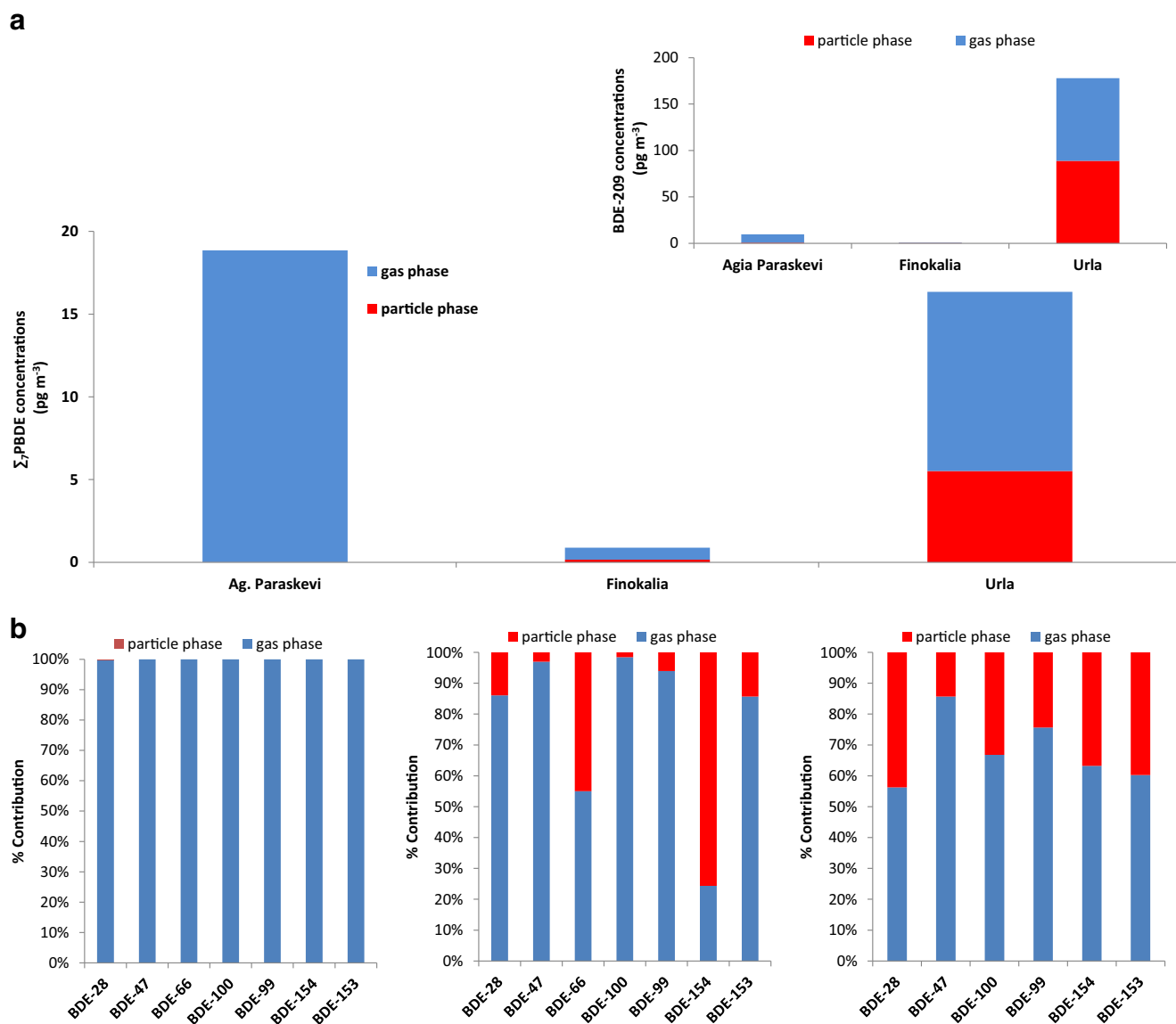
Fig. 1 **a** Average concentrations of $\sum_7$PBDE and BDE-209 in gas and particle phase (pg m^{-3}) and **b** distribution (%) between gas and particle phase for PBDE congeners at the three sampling sites

Temperature dependence of the gas-phase PBDE concentrations

The temperature dependence of the gas-phase PBDE concentrations was investigated using Clausius–Clapeyron plots seperately for day and night samples (Fig. S1). A good linear reverse relationship between ln$P$ (gas-phase partial pressure, atm) and $1/T$ (average atmospheric temperature, K) could be observed at Ag. Paraskevi for all PBDE congeners except BDE-209. The slopes (m) were generally steep for day and night samples (Fig. S1) suggesting that the gas-phase PBDE levels at this site were influenced by short-range transport (Cetin and Odabasi 2008). At Finokalia, the ln$P - 1/T$ relationship was significant only for the hexa-brominated BDE-154 and BDE-153 showing more shallow negative slopes, whereas positive slopes were found for the

less brominated congeners. Lastly, at Urla, the gas-phase concentrations of all PBDE congeners exhibited very poor temperature dependence except BDE-28 during daytime. One possible explanation for the poor correlations could be that the effect of temperature is probably masked by other variables like wind speed and mixing height that are higher during daytime diluting the emissions from contaminated terrestrial surfaces and lower during the nighttime when emissions decrease and lower temperature and wind speed result to poor dispersion conditions.

G/P partitioning behavior

It has been shown (Finizio et al. 1997; Harner and Bidleman 1998; Pankow 1998) that both mechanisms driving the G/P partitioning of SOCs (adsorption onto particle surface and
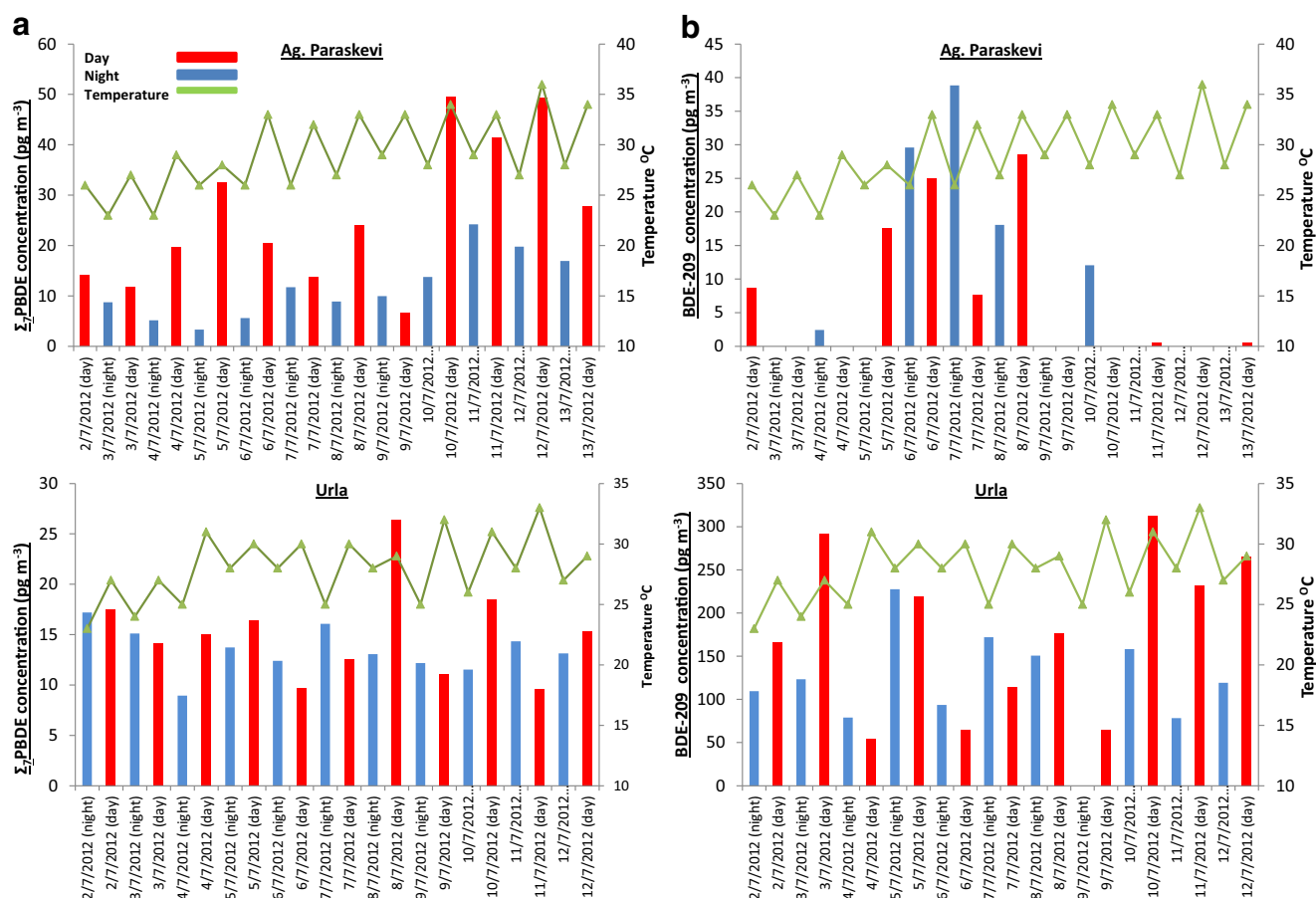
Fig. 2 Concentrations (pg m^{-3}) of $\sum_7$PBDE (**a**) and BDE-209 (**b**) in daytime and nighttime samples at Ag. Paraskevi and Urla

absorption into particle's organic matter) lead to a similar linear relationship between log K_P and log $P_L°$ of the compound according to Eq. (2). Furthermore, a linear relationship has been shown between log K_P and log K_{OA} (Eq. (4)) assuming absorption as the dominant process and octanol equivalence to the sorbing organic matter in particles (Harner and Bidleman 1998; Pankow 1987). In a recent study, Li et al. (2015) established a steady-state model (Eq. (7)) for the investigation of the G/P partitioning behavior of PBDEs and found that the K_{OA} model extended to cover steady-state is superior to the conventional (equilibrium) K_{OA} model.

Figure 3 presents the regression plots of log K_P vs. log $P_L°$ and log K_{OA} for BDE-47, BDE-100, BDE-99, BDE-154, BDE-153, and BDE-209 at Finokalia and Urla. Significant linear log K_P-log $P_L°$ correlations could be observed at Finokalia and Urla with R^2 values 0.849 ($p < 0.05$) and 0.86 ($p < 0.05$), respectively (Fig. 3a). A steeper slope (m) was observed at Finokalia (-0.2), close to the values reported for sites in Turkey (-0.2 to -0.22, Cetin and Odabasi 2008) and Italy (-0.2 to -0.22, Cincinelli et al. 2014) and higher than the values found at sites in northern Greece (-0.4 to -0.5, Besis et al. 2016) and China (-0.6, Chen et al. 2006; -0.02 to -0.8, Li and Jia 2014). By contrast, the slope at Urla was shallower (-0.1). The slopes derived from monitoring data often deviate from -1, possibly because of

sampling artifacts and/or non-equilibrium conditions or thermodynamic factors (Cetin and Odabasi 2008; Chen et al. 2006; Yang et al. 2013). The value of intercept b at Finokalia (-3.2) was comparable with those reported by Besis et al. (2016) at an urban background site in Thessaloniki (-4.5) and at an urban site in Turkey (-4.5) (Cetin and Odabasi 2008), whereas a higher b value was found at Urla (-2.2).

Good linear relationships were also obtained between log K_P and log K_{OA} with R^2 values 0.832 ($p < 0.05$) and 0.868 ($p < 0.05$) at Finokalia and Urla, respectively (Fig. 3b). The regression slope (m) was 0.3 at Finokalia, relatively lower than those reported for sites in northern Greece (0.6–0.7, Besis et al. 2016), and 0.1 at Urla, relatively lower than those reported for sites in Turkey (0.3–0.5, Cetin and Odabasi 2008). At both sampling sites, m deviated largely from 1 suggesting that sorption to aerosol particles was affected by molecular interactions different from those governing sorption to an octanol phase or that phase equilibrium was not established.

Prediction of particulate mass fraction Φ

Figure 4a presents the observed Φ values (Φ$_{exper}$) in comparison to those predicted (Φ$_{pred}$) by the J–P adsorption model. Relatively good agreement was obtained for BDE-28 and

Fig. 3 Plots of log K_P (m^3 μg^{-1}) measured at Finokalia and Urla vs. (**a**) log $P_L°$ (Pa) and (**b**) log K_{OA} for BDE-47, BDE-100, BDE-99, BDE-154, BDE-153, and BDE-209 (shared PBDE congeners at two sampling sites; only samples with concentrations > LOQ in both the gas and particulate phases were used to calculate the average value)
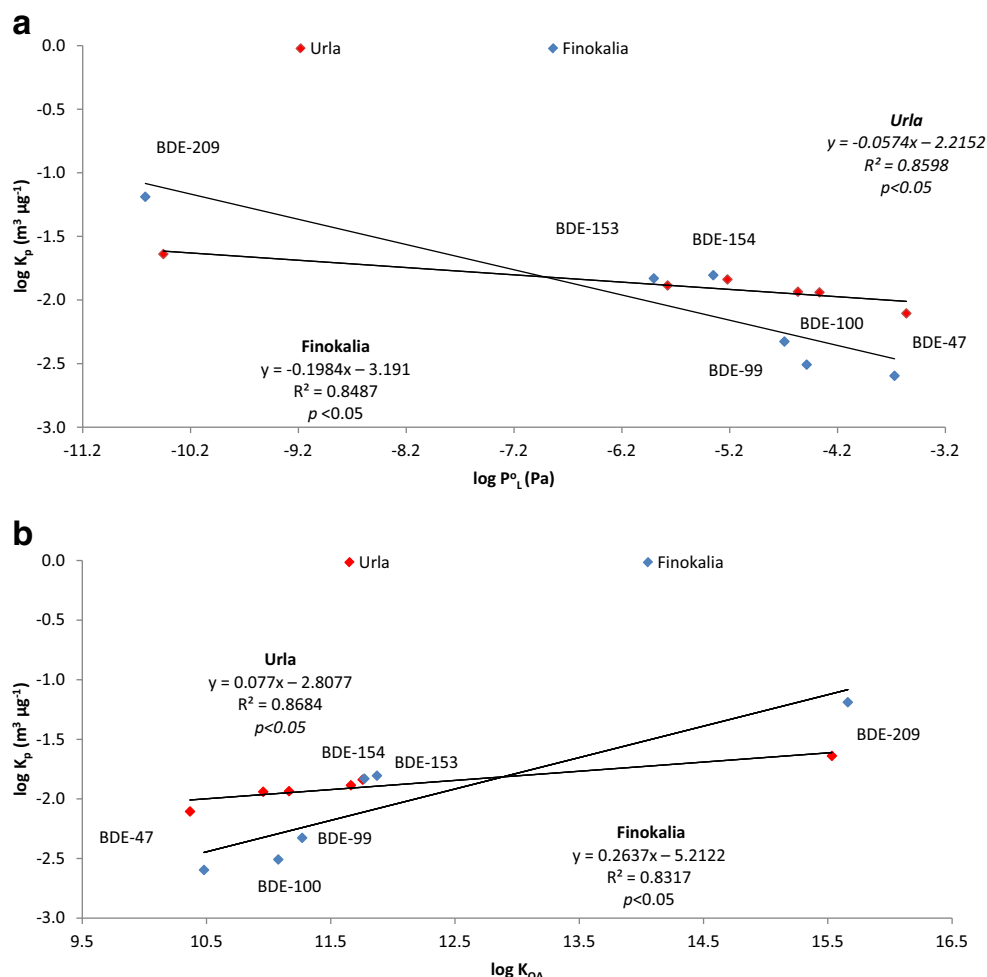
BDE-154 at Finokalia and for BDE-28 at Urla, though the model significantly overestimated the sorption of BDE-49, BDE-99, BDE-100, and BDE-209 at both sites. As the observed Φ values are not significantly influenced by vapor pressure, the adsorption model obviously fails to capture the significant partition processes. Similar overestimation has also been found in other studies (Chen et al. 2006; Cincinelli et al. 2014).

Figure 4b presents Φ_{exper} in comparison to Φ_{pred} derived by the conventional K_{OA} model. Absorption in organic matter is predicted to be significant for G/P partitioning of PBDEs, with the exception of BDE-28, which, however, is found to partition to a significant extent at Urla. Furthermore, the absorption model assuming equilibrium tends to overpredict the partitioning of all other BDEs at the two sites, except BDE-47 at Urla. Cetin and Odabasi (2008) also found the K_{OA} model to overestimate Φ of PBDEs (with the exception of BDE-28) and suggested mass transfer kinetic limitations (dynamic uptake model) to explain deviation from phase equilibrium, (later confirmed by the application of the K_{OA} model under steady state; Li et al. 2015). Kinetic limitations might explain these differences in the phase partitioning at Finokalia: Reduced availability of organic matter for G/P partitioning could result from burial or coating

(shell-like particles) by secondary inorganic or organic aerosol or, eventually, cloud-processed mineral dust. At Urla, the best agreement between Φ_{exper} and Φ_{pred} was found for f_{om} 10 and 20% for all congeners excepting BDE-47 and BDE-28 that exhibited best agreement at f_{om} 55%.

Figure 4c presents Φ_{exper} in comparison to Φ_{pred} derived by the steady-state model. Quite good agreement could be observed for most PBDE congeners at Urla. By contrast, at Finokalia, the steady-state model overpredicted Φ for BDE-47, BDE-99, BDE-100, and BDE-153, while underpredicting Φ for BDE-66 and BDE-154. It is worth to note that, at both sites, the best fit to experimental Φ was found for BDE-209. Higher brominated BDEs are not expected to be in phase equilibrium as relaxation to disturbances from deposition of gas phase compounds onto particles (or, eventual, re-volatilization) is slow. According to Li et al. (2015), in background air (and TSP < 30 μg m^{-3}), the maximum Φ of PBDE congeners should not exceed ≈ 50% under steady state. Therefore, the Φ of BDEs with > 4 Br atoms should be lower in air masses recently influenced by emissions or deposition processes. In our data sets, Φ was > 0.5 for BDE-154 and BDE-209 in at least some of the samples (at both sites). In similarity to the equilibrium-state model, the best agreement
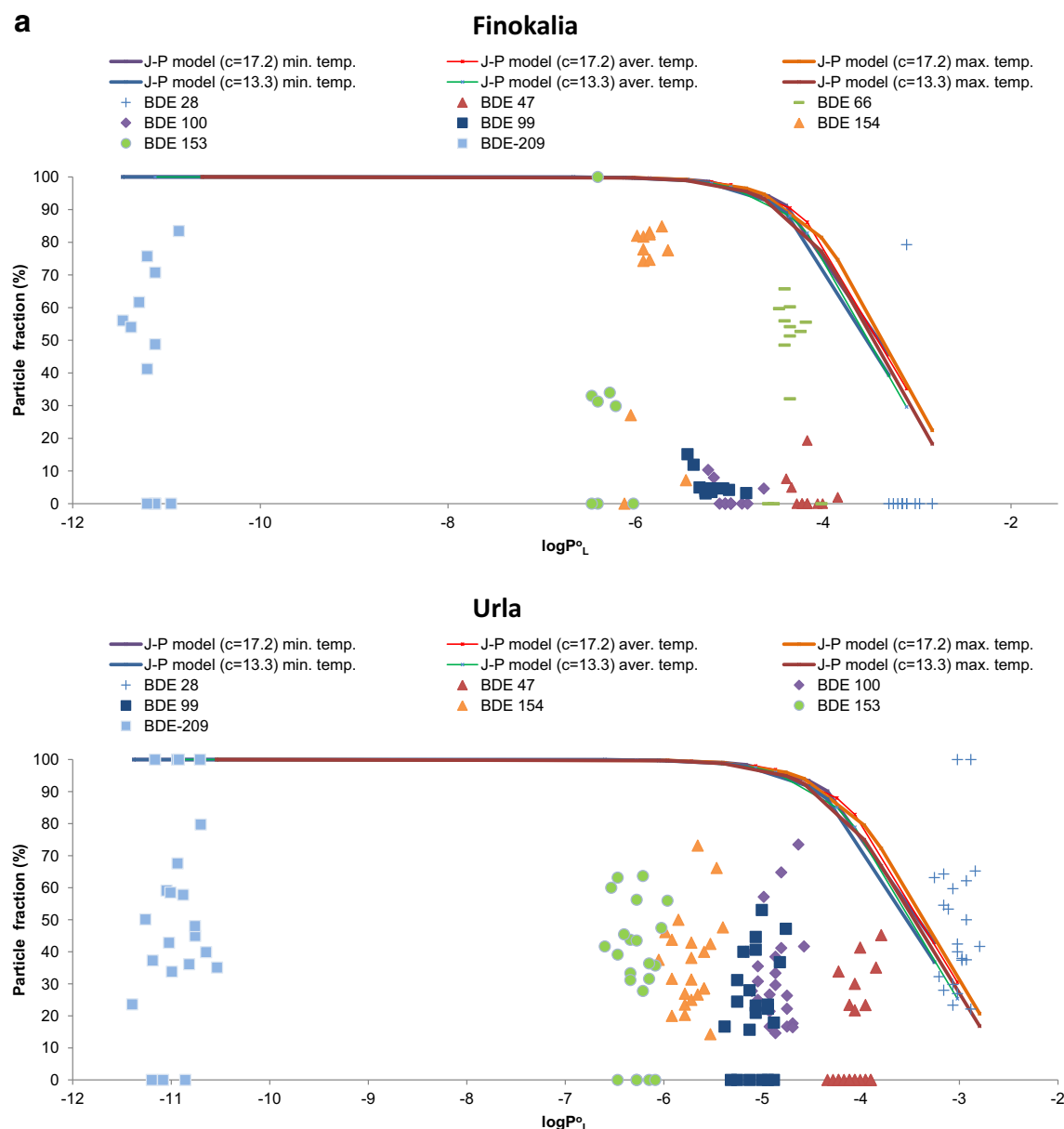
Fig. 4 Comparison of the measured particulate fractions ($\Phi \times 100\%$) of PBDEs with **a** predictions of the Junge–Pankow adsorption model ($c = 17.2$ and 13.3 Pa cm, $\theta = 7.7 \pm 1.5 \times 10^{-5}$ cm^2 cm^{-3}) and predictions of the (K_{OA-}) absorption model under **b** equilibrium (Harner–Bidleman model) and **c** under steady state (Li–Ma–Yang model), with 13% (min), 23% (mean), and 29% (max) organic matters at Finokalia and 10, 20, and 55% of organic matters at Urla (K_{OA}-based absorption model and steady-state model for minimum, mean, and maximum temperatures)

between Φ_{exper} and Φ_{pred} obtained by the steady-state model in Urla was found for f_{om} 10 and 20% for all congeners except BDE-47 and BDE-28.

In general, PBDE particulate mass fractions were similar for the same congeners at Finokalia (as found in earlier studies, e.g., Cetin and Odabasi 2008), while they scattered largely for individual congeners at the rural/coastal site Urla. This points to non-equilibrium conditions, eventually related to fresh emissions, which was actually shown to be the case in AIA (Cetin and Odabasi 2008; Odabasi et al. 2009; Odabasi et al. 2015a; Odabasi et al. 2015b).

The Φ_{exper}/Φ_{pred} ratio values derived from the three models are comparatively presented in Fig. 5 and Table S5. The steady-state model obviously appeared to better predict the observed Φ values for BDE-209 at Finokalia and Urla with Φ_{exper}/Φ_{pred} ratio values 0.8 and 1, respectively, in line with the expectation that equilibrium is least achieved under low PM levels. The steady-state model was also superior for BDE-153 and BDE-154 at Urla, while being comparable to the absorption equilibrium-state model for BDE-47, BDE-99, and BDE-100. At Finokalia, the conventional K_{OA} model was comparable or slightly better than the steady-state model
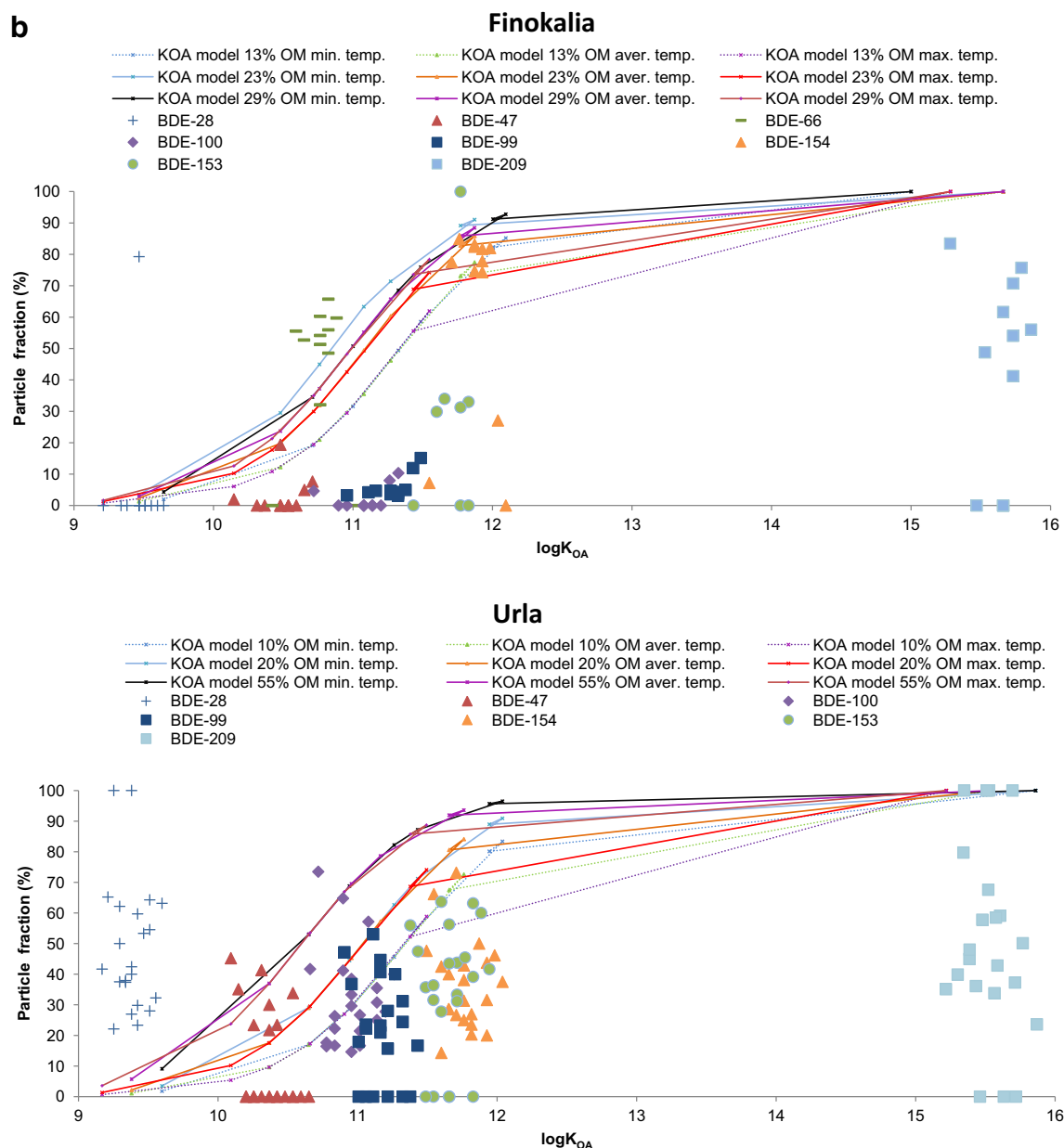
Fig. 4 (continued)

for BDE-66 and BDE-154. These results are in general agreement to Li et al. (2015), who suggested that the higher brominated BDEs (> 4 Br homologs) are not expected to be in phase equilibrium as relaxation to disturbances from deposition (or, eventual, re-volatilization) should be slow. Therefore, the particulate mass fraction of BDEs with > 4 Br atoms should be lower in air masses recently influenced by emissions.

On the other hand, the performance of the steady-state model was not better for BDE-153 and BDE-154 at Finokalia unlike for sites in China (Li et al. 2015). The reason could be that, ideally, the individual samples' aerosol characteristics and history, rather than the data subset's mean values, should be input to the steady-state model, i.e., PBDE source

and sink terms, and parameter C (see the "Calculations of G/P partition parameters" section), which is a measure of the boundary layer thickness to be penetrated by phase changing molecules. Also, the apparent sink "burial" in particles, which may inhibit G/P partitioning (Zhou et al. 2012; Zhou et al. 2013), might have occurred in individual samples' histories.

Particle-size distribution of PBDEs

Mean aggregate concentrations (sum of all particle fractions) of $\sum_7$PBDE at Neochorouda and Finokalia were found to be 1.04 and 0.13 pg m^{-3}, respectively (Table S6), lower than $\sum_{12}$PBDE (including the same congeners plus BDE-15,
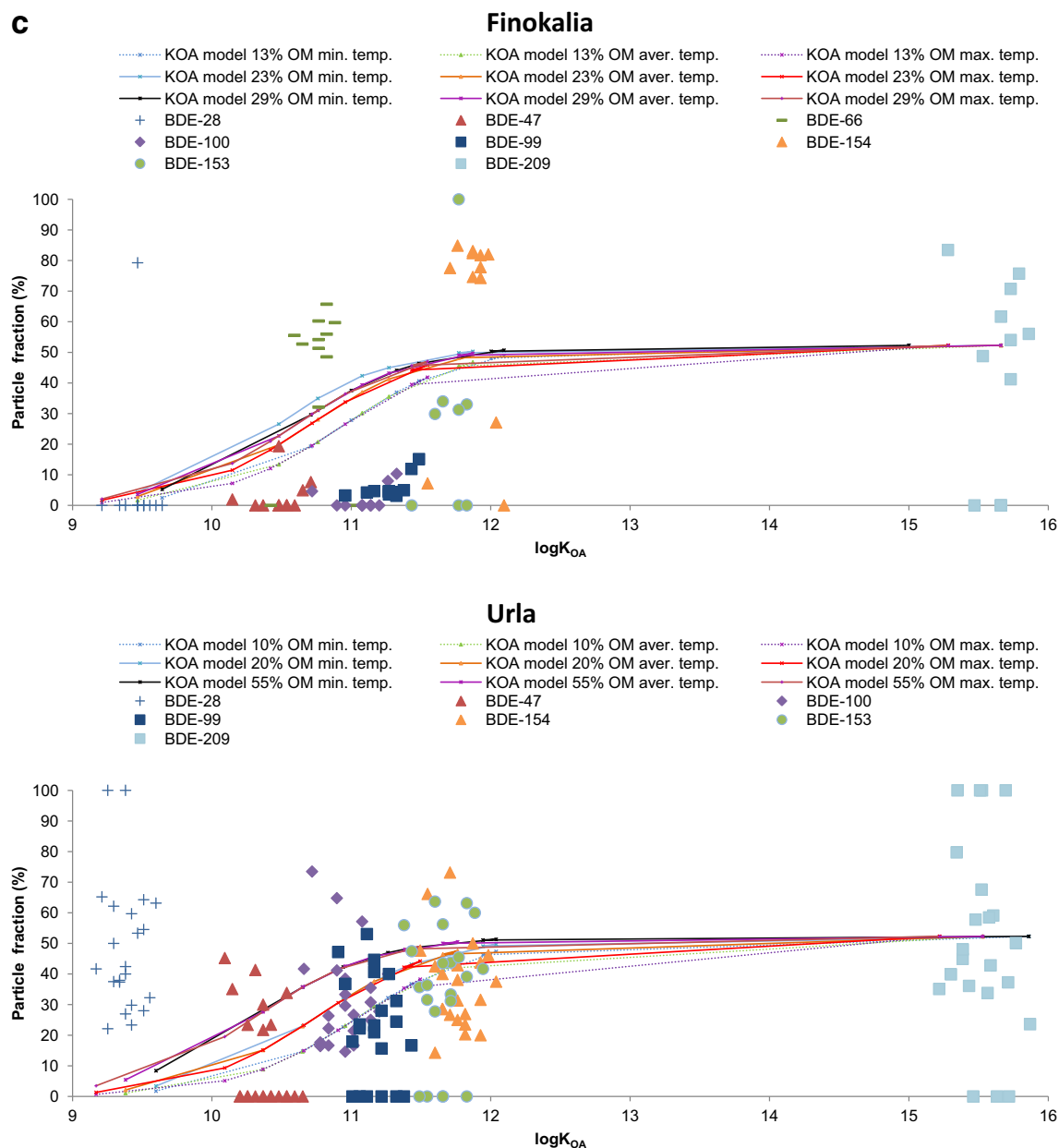
Fig. 4 (continued)

BDE-17, BDE-49 + 71, and BDE-183) found in summer 2013 at an urban background site and a heavy traffic site of the nearby urban agglomeration of Thessaloniki (2.4 and 27.1 pg m^{-3}, respectively, Besis et al. 2015). Mean aggregate concentrations found at the two sites are in close agreement with particle-bound concentrations of $\sum_{12}$PBDE found in the suburbs of Heraklion and at Finokalia (1.3 and 0.2–0.4 pg m^{-3}, respectively, Mandalakis et al. 2009). Average BDE-209 concentrations were seven and two times higher than $\sum_7$PBDE concentrations at Neochorouda and Finokalia, respectively, (Table S6).

The size distribution of $\sum_7$PBDE and BDE-209 is shown in Fig. 6. For comparison reasons, particle size fractions < 0.49

and 0.49–0.95 μm from Finokalia were merged. The size distribution of $\sum_7$PBDEs at the two sites featured a distinct enrichment in the submicron particles particularly at Neochorouda where 69% on average of the total mass was associated with particles < 0.95 μm. A shift in the abundances of $\sum_7$PBDE toward larger particles could be observed at Finokalia with 38% of the total mass in the submicrometric fraction and 18% in the coarse fraction (> 7.2 μm). The enrichment of PBDEs in the finest particle fraction has significant implications for their atmospheric fate considering that the removal mechanisms of aerosol from the atmosphere (wet and dry deposition) are less efficient for smaller particles; therefore, fine aerosols have long residence times and are largely susceptible to long-range

Fig. 5 Ratio of Φ experimental and Φ predicted from the J–P model, the (K_{OA}-) absorption model under equilibrium and under steady-state model
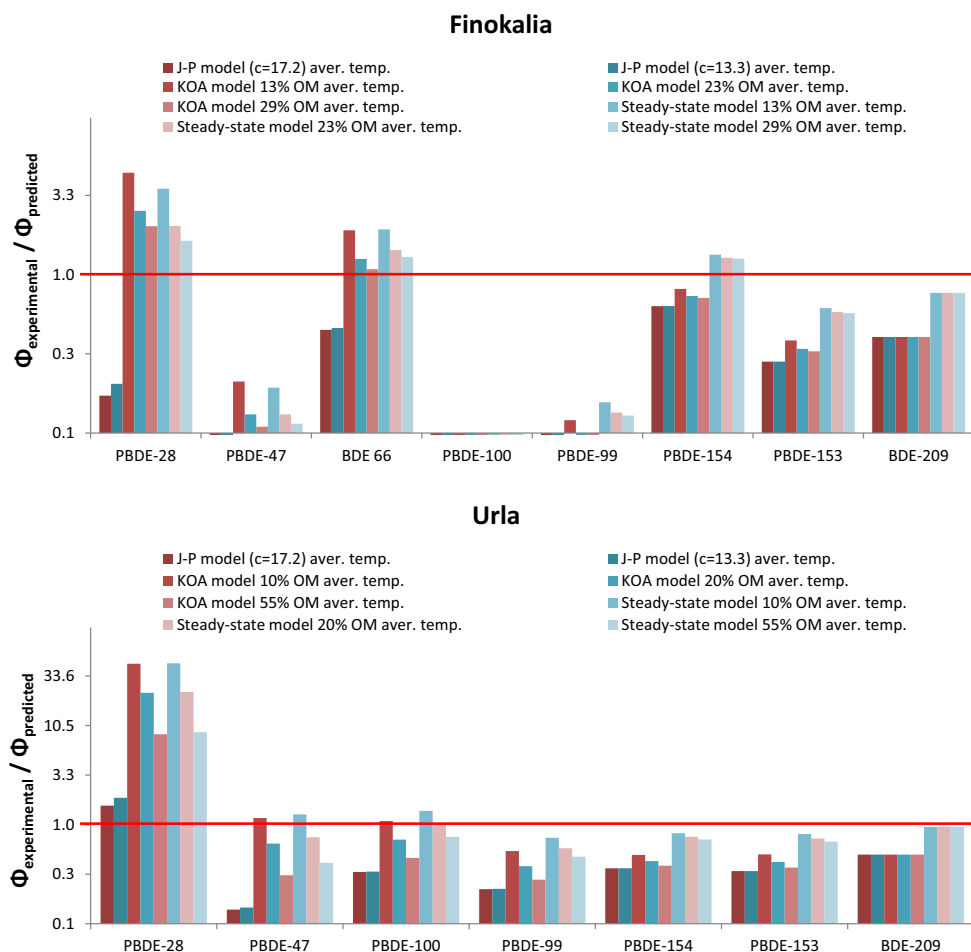
transport. Moreover, the size distribution of PBDEs has a decisive influence on their potential health effects considering that particles < 0.95 μm penetrate into the deepest parts of the respiratory system, the alveoli; therefore, PBDEs bound to this fraction may pose a great risk to human health.

The size distribution of individual PBDE congeners depended on their molecular weight, with the low-molecular weight PBDE congeners being associated mostly with particles > 0.95 μm, whereas the less volatile heavier congeners BDEs 99, 100, 153, and 154 being mainly bound to submicron particles (Fig. S2). Analogous trends have also been observed for PBDEs (Besis et al. 2015; Luo et al. 2014; Lyu et al. 2016; Mandalakis et al. 2009; Okonski et al. 2014) and other classes of organic contaminants (Chrysikou and Samara 2009; Landlová et al. 2014). BDE-209 exhibited a different size distribution pattern (Fig. S2) exhibiting an appreciable fraction in coarse particles > 3 μm (55 and 52% at Neochorouda and Finokalia, respectively). Apparently, lower brominated and more volatile congeners (tri- to hexa-BDEs), partitioning between gas and particulate phase, may redistribute among different-sized particles. By contrast, heavily brominated congeners (hepta- to deca-BDEs) that are predominant in the particle phase tend to stay on the particles they get sorbed to.

Theoretically, heavily brominated congeners are expected to affiliate with fine particles with large surface areas because of their strong hydrophobicity (La Guardia et al. 2006). The considerable affiliation of BDE-209 with coarse particles observed in the present study is likely related to the fact that, as reported in the "G/P partitioning behavior" section, it did not relax to phase equilibrium due to slow mass transfer (Li et al. 2015; Luo et al. 2014).

The mean normalized size distribution of PBDEs (dC/dlogDp vs. logDp) is presented in Fig. 7. Concerning ∑7PBDE, a bimodal distribution is evident at Neochorouda with a major peak in the accumulation mode (< 0.95 μm) and a minor peak in the coarse mode (3–7.2 μm). Bimodal distributions for ∑PBDE with peaks in submicron and coarse particles were also reported by other investigators (Mandalakis et al. 2009 for Heraklion, Crete; Zhang et al. 2012 for urban Guangzhou, China); by contrast, a unimodal distribution was found at traffic and urban background sites in Thessaloniki, northern Greece peaking at 0.49–0.97 μm with a shift to larger particles 0.97–1.5 μm in summer (Besis et al. 2015). ∑7PBDE exhibited a unimodal distribution at Finokalia, peaking in 0.95–1.5 μm. Given that the highest peak in ∑7PBDE is usually observed in the finest fraction, this shift toward the 0.49–
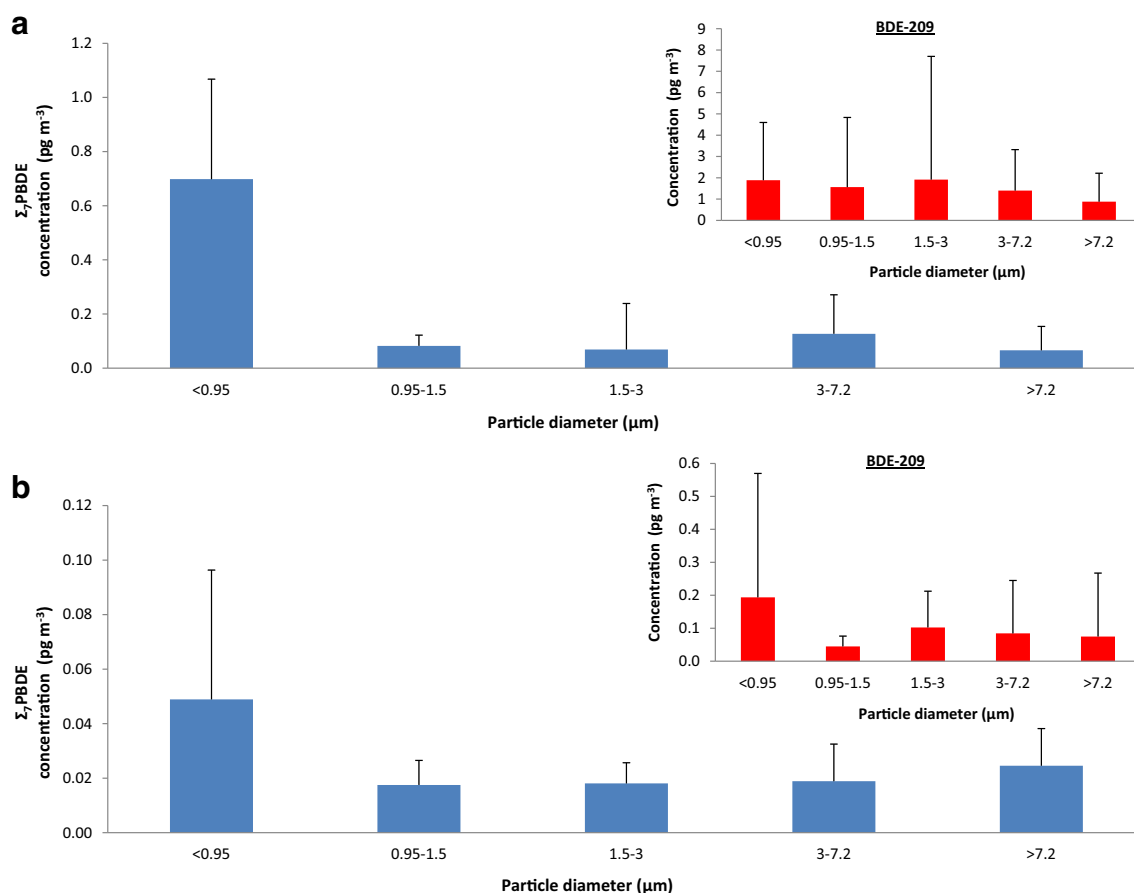
Fig. 6 Average concentrations of $\sum_7$PBDE and BDE-209 in various size fractions. **a** Neochorouda. **b** Finokalia. (Error bars show min, max)

0.95 μm size fraction may be due to the shift in PM distribution caused by aging of aerosols at this site (Okonski et al. 2014). Similarly to an urban site in Brno, Czech Republic (Okonski et al. 2014), all tri- to octa-BDEs at Neochorouda exhibited bimodal distributions with BDE-28, BDE-66, BDE-154, and BDE-153 having the most significant occurrence in the coarse mode, likely due to redistribution of the more volatile congeners from smaller size fractions to available coarse aerosols (La Guardia et al. 2006; Wang et al. 2008). The same congeners exhibited a significant coarse fraction (> 7.2 μm) also at Finokalia in contrast to BDE-47, BDE-99, and BDE-100 that showed a unimodal distribution peaking at 0.95–1.5 μm. BDE-209 exhibited unimodal distribution at both sites with peak in 0.95–1.5 μm at Neochorouda, similar to Luo et al. (2014) (1–1.8 μm), and in larger particles (1.5–3 μm) at Finokalia.

The mass median aerodynamic diameter (the particle size below which 50% of the particle population lies on the basis of mass; MMAD) of PBDEs was calculated from cumulative distribution percentages according to O'Shaughnessy and Raabe (2003). The MMADs of $\sum_7$PBDE at Neochorouda and Finokalia were 0.67 ± 0.25 and 0.87 ± 0.19 μm, respectively. The MMADs of individual PBDE congeners (1.69 ± 0.22, 0.73 ± 0.33, 0.71 ± 0.32, 0.35 ± 0.25 at

Neochorouda vs. 0.92 ± 0.42, 0.84 ± 0.03, 0.81 ± 0.17, 0.80 ± 0.14 at Finokalia, for BDE-28, BDE-47, BDE-99, and BDE-100, respectively) reflect the tendency of the more volatile congeners to re-distribute in the aerosol across particle sizes, while the higher and less volatile congeners are restricted to the submicrometer particles even during long-range transport. For BDE-154 and BDE-153, the MMADs were 1.65 ± 0.01 and 1.40 ± 0.14 at Neochorouda and in the same range with those calculated at Finokalia (1.64 ± 1.17, 1.30 ± 1.82, respectively). The MMADs of BDE-209 were 1.99 ± 0.41 and 1.79 ± 0.45 at Neochorouda and Finokalia, respectively, indicating a relatively longer atmospheric residence time at the latter.

A significant positive correlation ($p < 0.05$) was obtained between MMADs and log $P_L°$ for the less brominated congeners BDE-28, BDE-47, BDE-100, and BDE-99 at both sites, Neochorouda ($R^2 = 0.886$) and Finokalia ($R^2 = 0.955$). By contrast, a negative correlation was observed for the higher brominated congeners (BDE-154, BDE-153, and BDE-209) that was statistically significant only at Neochorouda ($R^2 = 0.749$, $p < 0.05$) (Fig. 8). Luo et al. (2014) reported positive correlation between mass fractions in coarse particles and the log $P_L°$ for tri- to hexa-BDEs, and a negative correlation for hepta- to deca-BDEs. Also, Lyu et al. (2016) reported a moderate positive
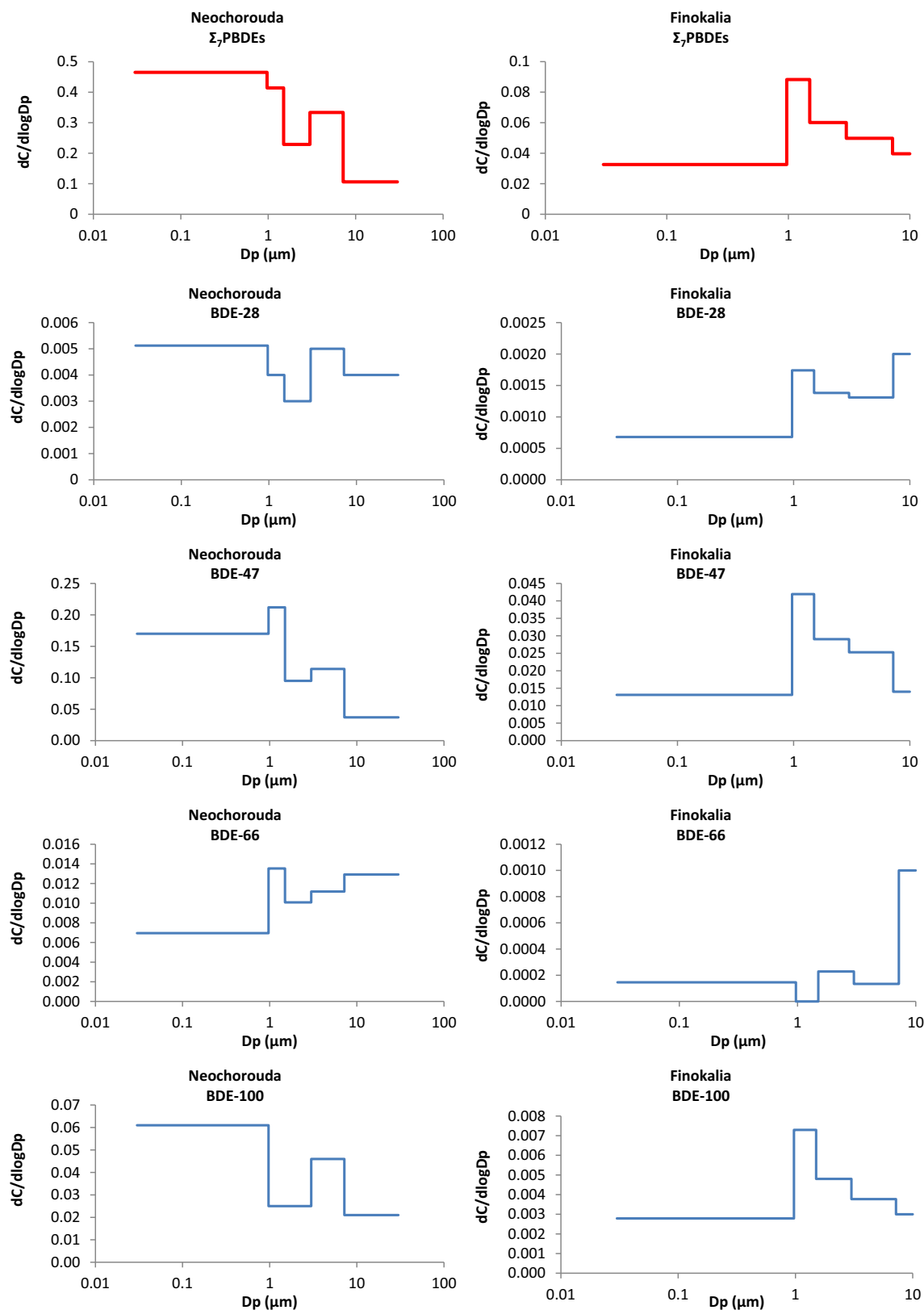
Fig. 7 Normalized size distribution of $\sum_7$PBDE and individual PBDE congener at Neochorouda and Finokalia

correlation between geometric mass diameter (GMD) and log $P_L°$ for PBDEs excluding BDE-209. Finally, mass fractions of

PBDEs in the coarse mode particles decreased as their volatilities decreased in Zhang et al. (2012). Migration of the more
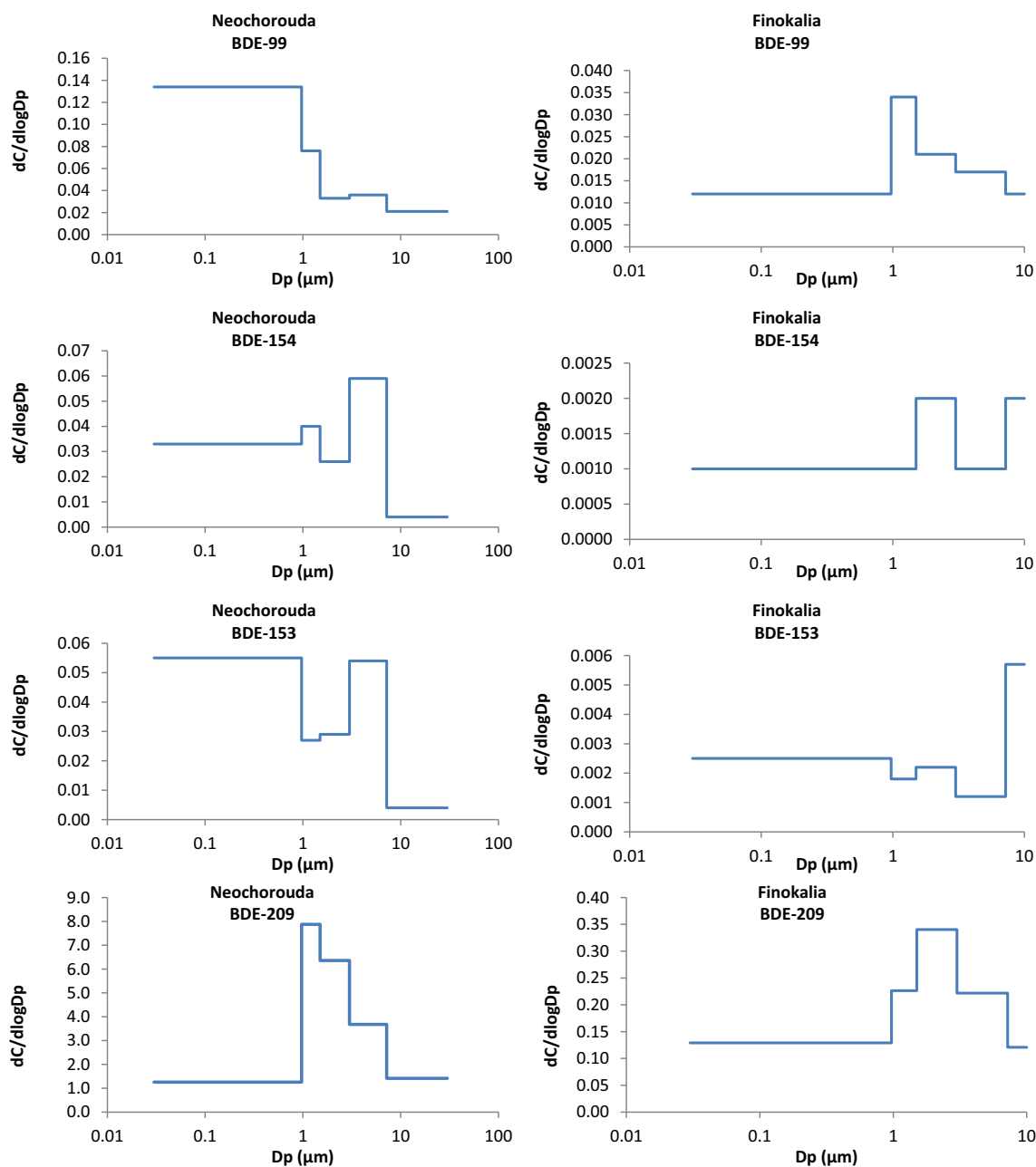
Fig. 7 (continued)

volatile PBDEs to larger particles through volatilization and condensation as well as differences in chemical affinities between individual PBDEs and different size particles are plausible mechanisms for the relatively large mass fractions in the coarse particle mode.

Congener profile and potential sources

A clear prevalence of BDE-209 compared to $\sum_7$PBDE was observed at Urla suggesting in-use emissions of the deca-BDE commercial mixture (Table 1), while BDE-209 and $\sum_7$PBDE concentrations were almost equal at Ag. Paraskevi and

Finokalia. BDE-209-dominated profiles were also reported for the close-by AIA and for Izmir (Cetin and Odabasi 2008; Odabasi et al. 2009, 2015a, b).

In both atmospheric phases, the dominant congeners in $\sum_7$PBDE were BDE-47 and BDE-99 (Fig. S3). The mean BDE-47/BDE-99 ratio in total (G + P) phase was 3.3 at Ag. Paraskevi, 2.2 at Finokalia, and 1.5 at Urla. The corresponding ratios in the size-segregated particle samples were 1.5 at Neochorouda and 1.8 at Finokalia on average. These values are quite higher than those reported for Bromkal 70-5DE technical formulation (0.96) (La Guardia et al. 2006) suggesting possible thermal or photolytic degradation of BDE-209 to
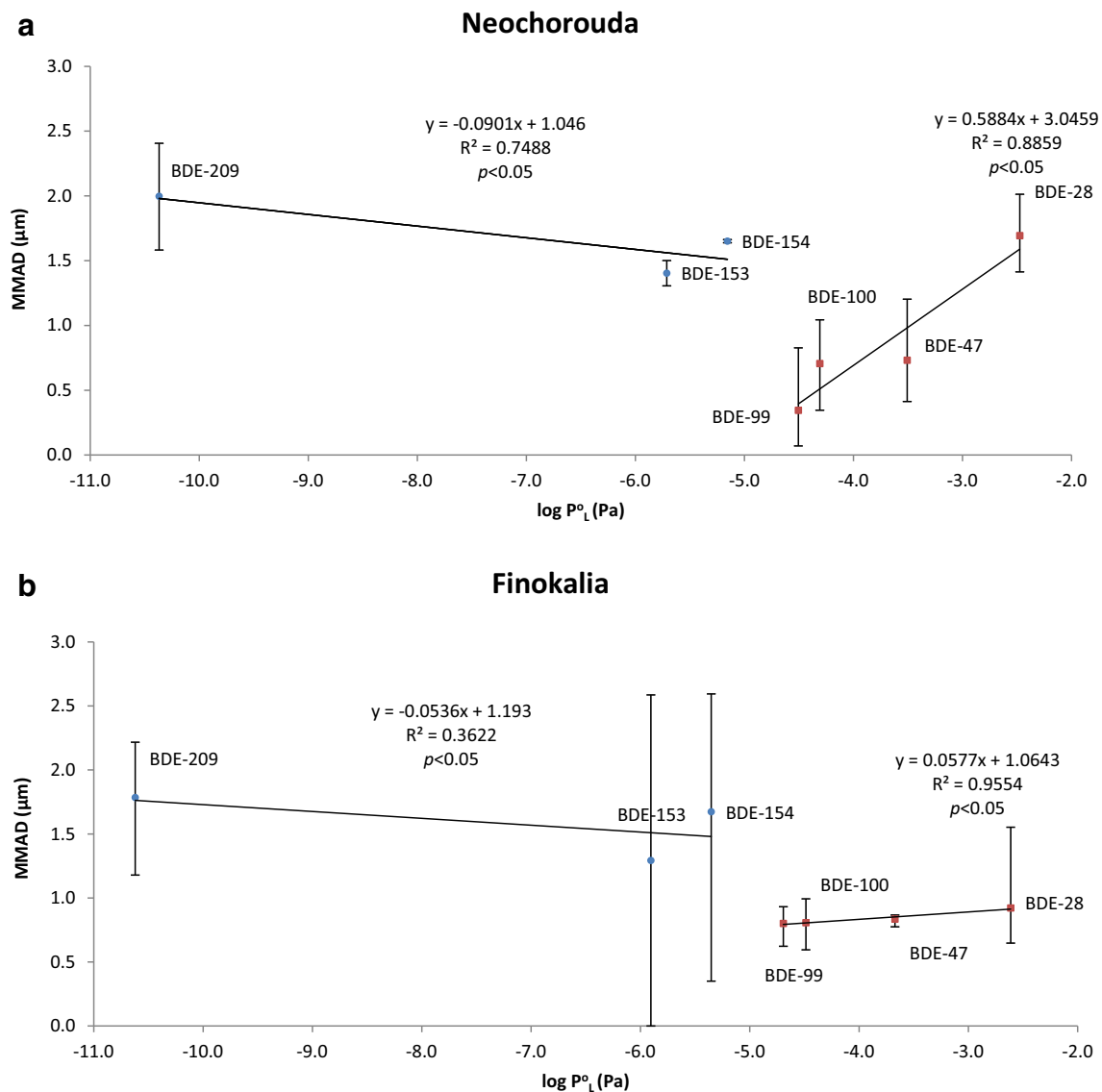
a
Neochorouda

b
Finokalia

Fig. 8 Plots of MMADs vs. log $P_L°$ for BDE-28, BDE-47, BDE-100, BDE-99, BDE-154, BDE-153, and BDE-209 at **a** Neochorouda and **b** Finokalia (error bars show min, max)

lower congeners including BDE-47 and BDE-99 (Bezares-Cruz et al. 2004).

Long-range transport

The potential source regions of PBDEs were identified by calculating the 3-day (72-h) back-trajectories of air masses at altitudes above 500 m using the HYSPLIT model developed by the National Oceanic and Atmospheric Administration (NOAA). The backward trajectory analysis (Fig. S4) showed that air masses arriving at Urla, Finokalia, and Ag. Paraskevi during the sampling campaign originated mostly from the northeastern sector (Russia and Black Sea). Air masses advected to Urla might have picked up pollution while passing over the industrial area of Aliaga (50 km to north-northeast), and/or over the Istanbul–Izmit urban and industrial area (350–

400 km, Cetin and Odabasi 2007b, 2008) and could explain the higher concentrations of BDE-209 at Urla. Air masses advected to Ag. Paraskevi also might have been affected by emissions in the Istanbul-Izmit area. However, advection of air pollution from the center of Athens and the heavily industrialized Thriassion Plain located at distances 10–35 km to southwest as a result of the sea breeze circulation is more likely to occur during daytime. Advection was analyzed more thoroughly for the remote site Finokalia located some 70 km east of the Heraklion city (100,000 inhabitants). It received long-range transported air pollution only occasionally during the measurements, mostly from the Izmir urban area if at all, whereas otherwise, the air represents the clean background of the Aegean. The pollution contribution to individual samples collected at Finokalia was quantified as an urban dose the air masses had experienced (Lammel et al. 2016), based on

inverse dispersion modeling (using the FLEXPART model; Stohl et al. 2005). A comparison of each three samples collecting background (minimal urban dose attributed to samples) or influence of urban pollution (maximal dose) shows PBDEs by average a factor of 2 (2.0 ± 1.2) higher under urban influence than under background conditions.

Differently to the other sampling sites, air masses approaching Neochorouda during the sampling campaign originated mostly from the northern sector (central and eastern Europe) excepting one sampling event (July 12, 2012) that was associated with air masses from the western sector (Spain, western Mediterranean Sea). Therefore, some long-range transport from Central and Eastern Europe could be assumed in combination to local emissions transported by the local sea–land breeze system from the urban and industrial parts of the nearby Thessaloniki conurbation (more than 1,000,000 inhabitants) located upwind during nighttime. Furthermore, air mass stagnation is not unlikely under anticyclonic conditions in the area of Thessaloniki (Samara et al. 2014).

Conclusions

The G/P partitioning behavior of PBDEs and their particle-size distribution were investigated at background sites around the Aegean Sea during summertime. Significant linear log K_P vs. log $P_L°$ and log K_P vs. log K_{OA} relationships were observed; however, the slope values implied lack of equilibrium. The big scatter of PBDE particulate mass fraction, Φ, observed in particular at the rural coastal site, points to non-equilibrium conditions, eventually caused by fresh emissions or fluctuating sinks. Indeed, a steady-state G/P partitioning model appeared to relatively better predict the observed Φ values for BDE-209 in comparison to the adsorption and the absorption equilibrium models. This successful application of an absorption (K_{OA}) model under steady state confirms the perception that relaxation to equilibrium should be slowest under clean/low PM conditions. Despite the differences discerned between congeners, the largest mass of total particle-bound $\sum_7$PBDE was found associated with the submicrometer particle fraction. This means that PBDEs may have long atmospheric residence time (days to weeks in dry periods; Ruijgrok et al. 1995) and reach the deeper parts of the human respiratory system. BDE-209 exhibited a different size distribution pattern with appreciable percentage (52–55%) in the coarse particle fraction (> 3 μm). A positive correlation between MMADs and log $P_L°$ was obtained for less brominated congeners (BDE-28, BDE-47, BDE-100, and BDE-99) that can explain the relatively higher abundance of more volatile PBDEs in the coarse particle mode. For heavily brominated congeners, a negative correlation was observed between MMADs and log $P_L°$, which in the case of BDE-

209 could be explained by the lack of equilibrium. Air mass trajectory analysis revealed that long-range transport was likely for all sites; however, the high concentrations of BDE-209 at Urla indicate influence from short distance sources. Overall, although the findings of the present study improve our understanding on the phase partitioning and the size distribution of PBDEs, the atmospheric behavior of these compounds in background air deserves further investigation.

References

Besis A, Botsaropoulou E, Voutsa D, Samara C (2015) Particle-size distribution of polybrominated diphenyl ethers (PBDEs) in the urban agglomeration of Thessaloniki, northern Greece. Atmos Environ 104:176–185. https://doi.org/10.1016/j.atmosenv.2015.01.019

Besis A, Samara C (2012) Polybrominated diphenyl ethers (PBDEs) in the indoor and outdoor environments—a review on occurrence and human exposure. Environ Pollut 169:217–229. https://doi.org/10.1016/j.envpol.2012.04.009

Besis A, Voutsa D, Samara C (2016) Atmospheric occurrence and gas-particle partitioning of PBDEs at industrial, urban and suburban sites of Thessaloniki, northern Greece: implications for human health. Environ Pollut 215:113–124. https://doi.org/10.1016/j.envpol.2016.04.093

Bezares-Cruz J, Jafvert CT, Hua I (2004) Solar photodecomposition of decabromodiphenyl ether: products and quantum yield. Environ Sci Technol 38:4149–4156. https://doi.org/10.1021/es049608o

Cetin B, Odabasi M (2007a) Air–water exchange and dry deposition of polybrominated diphenyl ethers at a coastal site in Izmir Bay, Turkey. Environ Sci Technol 41:785–791. https://doi.org/10.1021/es061368k

Cetin B, Odabasi M (2007b) Particle-phase dry deposition and air–soil gas-exchange of polybrominated diphenyl ethers (PBDEs) in Izmir, Turkey. Environ Sci Technol 41:4986–4992. https://doi.org/10.1021/es070187v

Cetin B, Odabasi M (2008) Atmospheric concentrations and phase partitioning of polybrominated diphenyl ethers (PBDEs) in Izmir, Turkey. Chemosphere 71:1067–1078. https://doi.org/10.1016/j.chemosphere.2007.10.052

Cetin B, Odabasi M (2011) Polybrominated diphenyl ethers (PBDEs) in indoor and outdoor window organic films in Izmir, Turkey. J Hazard Mater 185:784–791. https://doi.org/10.1016/j.jhazmat.2010.09.089

Chao HR, Tsou TC, Huang HL, Chang-Chien GP (2011) Levels of breast milk PBDEs from southern taiwan and their potential impact on neurodevelopment. Pediatr Res 70:596–600. https://doi.org/10.1203/PDR.0b013e3182320b9b

Chen LG et al (2006) Concentration levels, compositional profiles, and gas-particle partitioning of polybrominated diphenyl ethers in the atmosphere of an urban city in South China. Environ Sci Technol 40:1190–1196. https://doi.org/10.1021/es052123v

Chrysikou LP, Samara CA (2009) Seasonal variation of the size distribution of urban particulate matter and associated organic pollutants in the ambient air. Atmos Environ 43:4557–4569. https://doi.org/10.1016/j.atmosenv.2009.06.033

Cincinelli A, Pieri F, Martellini T, Passaponti M, Del Bubba M, Del Vento S, Katsoyiannis AA (2014) Atmospheric occurrence and gas-particle partitioning of PBDEs in an industrialised and urban area of Florence, Italy. Aerosol Air Qual Res 14:1121–1130. https://doi.org/10.4209/aaqr.2013.01.0021

Darnerud PO, Eriksen GS, Jóhannesson T, Larsen PB, Viluksela M (2001) Polybrominated diphenyl ethers: occurrence, dietary exposure, and toxicology. Environ Health Perspect 109:49–68

Dayan U, Ricaud P, Zbinden R, Dulac F (2017) Atmospheric pollution concentrations over the Eastern Mediterranean during summer—a review. Atmos Chem Phys Discuss 2017:1–65. https://doi.org/10.5194/acp-2017-79

de Wit CA, Herzke D, Vorkamp K (2010) Brominated flame retardants in the Arctic environment—trends and new candidates. Sci Total Environ 408:2885–2918. https://doi.org/10.1016/j.scitotenv.2009.08.037

Finizio A, Mackay D, Bidleman T, Harner T (1997) Octanol-air partition coefficient as a predictor of partitioning of semi-volatile organic chemicals to aerosols. Atmos Environ 31:2289–2296. https://doi.org/10.1016/S1352-2310(97)00013-7

Gevao B et al (2013) Seasonal variations in the atmospheric concentrations of polybrominated diphenyl ethers in Kuwait. Sci Total Environ 454–455:534–541. https://doi.org/10.1016/j.scitotenv.2013.02.073

Harner T, Bidleman TF (1998) Octanol-air partition coefficient for describing particle/gas partitioning of aromatic compounds in urban air. Environ Sci Technol 32:1494–1502. https://doi.org/10.1021/es970890r

Harner T, Shoeib M (2002) Measurements of octanol–air partition coefficients (KOA) for polybrominated diphenyl ethers (PBDEs): predicting partitioning in the environment. J Chem Eng Data 47:228–232. https://doi.org/10.1021/je010192t

Harner T, Shoeib M, Diamond M, Ikonomou M, Stern G (2006) Passive sampler derived air concentrations of PBDEs along an urban–rural transect: spatial and temporal trends. Chemosphere 64:262–267. https://doi.org/10.1016/j.chemosphere.2005.12.018

He W et al (2014) Atmospheric PBDEs at rural and urban sites in central China from 2010 to 2013: residual levels, potential sources and human exposure. Environ Pollut 192:232–243. https://doi.org/10.1016/j.envpol.2014.03.014

La Guardia MJ, Hale RC, Harvey E (2006) Detailed polybrominated diphenyl ether (PBDE) congener composition of the widely used penta-, octa-, and deca-PBDE technical flame-retardant mixtures. Environ Sci Technol 40:6247–6254. https://doi.org/10.1021/es060630m

Lammel G et al (2015) Air and seawater pollution and air–sea gas exchange of persistent toxic substances in the Aegean Sea: spatial trends of PAHs, PCBs, OCPs and PBDEs. Environ Sci Pollut Res 22:11301–11313. https://doi.org/10.1007/s11356-015-4363-4

Lammel G, Mulder MD, Shahpoury P, Kukučka P, Lišková H, Přibylová P, Prokeš R, Wotawa G (2016). Nitropolyaromatic hydrocarbons—gas-particle partitioning, mass size distribution, and formation along transport in marine and continental background air in Europe, submitted

Landlová L, Čupr P, Franců J, Klánová J, Lammel G (2014) Composition and effects of inhalable size fractions of atmospheric aerosols in the polluted atmosphere: part I. PAHs, PCBs and OCPs and the matrix chemical composition. Environ Sci Pollut Res 21:6188–6204. https://doi.org/10.1007/s11356-014-2571-y

Li Y-F, Jia H-L (2014) Prediction of gas/particle partition quotients of polybrominated diphenyl ethers (PBDEs) in north temperate zone air: an empirical approach. Ecotoxicol Environ Saf 108:65–71. https://doi.org/10.1016/j.ecoenv.2014.05.028

Li YF, Ma WL, Yang M (2015) Prediction of gas/particle partitioning of polybrominated diphenyl ethers (PBDEs) in global air: a theoretical study. Atmos Chem Phys 15:1669–1681. https://doi.org/10.5194/acp-15-1669-2015

Li Y-F, Qiao L-N, Ren N-Q, Sverko E, Mackay D, Macdonald RW (2017) Decabrominated diphenyl ethers (BDE-209) in Chinese and global air: levels, gas/particle partitioning, and long-range transport: is long-range transport of BDE-209 really governed by the movement of particles? Environ Sci Technol 51:1035–1042. https://doi.org/10.1021/acs.est.6b05395

Luo P, Ni HG, Bao LJ, Li SM, Zeng EY (2014) Size distribution of airborne particle-bound polybrominated diphenyl ethers and its implications for dry and wet deposition Environ Sci Technol 48:13793–13799 doi:https://doi.org/10.1021/es5042018

Lyu Y, Xu T, Li X, Cheng T, Yang X, Sun X, Chen J (2016) Size distribution of particle-associated polybrominated diphenyl ethers (PBDEs) and their implications for health. Atmospheric Measurement Techniques 9:1025–1037. https://doi.org/10.5194/amt-9-1025-2016

Mandalakis M, Besis A, Stephanou EG (2009) Particle-size distribution and gas/particle partitioning of atmospheric polybrominated diphenyl ethers in urban areas of Greece. Environ Pollut 157:1227–1233. https://doi.org/10.1016/j.envpol.2008.12.010

Mulder MD, Heil A, Kukučka P, Kuta J, Přibylová P, Prokeš R, Lammel G (2015) Long-range atmospheric transport of PAHs, PCBs and PBDEs to the central and eastern Mediterranean and changes of PCB and PBDE congener patterns in summer 2010. Atmos Environ 111:51–59. https://doi.org/10.1016/j.atmosenv.2015.03.044

Odabasi M et al (2009) Electric arc furnaces for steel-making: hot spots for persistent organic pollutants. Environ Sci Technol 43:5205–5211. https://doi.org/10.1021/es900863s

Odabasi M et al (2015b) Biomonitoring the spatial and historical variations of persistent organic pollutants (POPs) in an industrial region. Environ Sci Technol 49:2105–2114. https://doi.org/10.1021/es506316t

Odabasi M, Cetin B, Bayram A (2015a) Persistent organic pollutants (POPs) on fine and coarse atmospheric particles measured at two (urban and industrial) sites. Aerosol Air Qual Res 15:1894–1905. https://doi.org/10.4209/aaqr.2015.02.0118

Okonski K et al (2014) Particle size distribution of halogenated flame retardants and implications for atmospheric deposition and transport. Environ Sci Technol 48:14426–14434. https://doi.org/10.1021/es5044547

O'Shaughnessy PT, Raabe OG (2003) A comparison of cascade impactor data reduction methods. Aerosol Sci Technol 37:187–200. https://doi.org/10.1080/02786820300956

Pankow JF (1987) Review and comparative analysis of the theories on partitioning between the gas and aerosol particulate phases in the atmosphere. Atmospheric Environment (1967) 21:2275–2283. https://doi.org/10.1016/0004-6981(87)90363-5

Pankow JF (1998) Further discussion of the octanol/air partition coefficient Koa as a correlating parameter for gas/particle partitioning coefficients. Atmos Environ 32:1493–1497. https://doi.org/10.1016/S1352-2310(97)00383-X

Ruijgrok W, Davidson CI, Nicholson KW (1995) Dry deposition of particles: implications and recommendations for mapping of deposition over Europe. Tellus Series B 47(B):587–601

Samara C, Voutsa D, Kouras A, Eleftheriadis K, Maggos T, Saraga D, Petrakakis M (2014) Organic and elemental carbon associated to

PM10 and PM2.5 at urban sites of northern Greece. Environ Sci Pollut Res 21:1769–1785. https://doi.org/10.1007/s11356-013-2052-8

Shy CG, Huang HL, Chao HR, Chang-Chien GP (2012) Cord blood levels of thyroid hormones and IGF-1 weakly correlate with breast milk levels of PBDEs in Taiwan. Int J Hyg Environ Health 215:345–351. https://doi.org/10.1016/j.ijheh.2011.10.004

Sofuoglu SC, Sofuoglu A, Holsen TM, Alexander CM, Pagano JJ (2013) Atmospheric concentrations and potential sources of PCBs, PBDEs, and pesticides to Acadia National Park. Environ Pollut 177:116–124. https://doi.org/10.1016/j.envpol.2013.02.015

Stohl A, Forster C, Frank A, Seibert P, Wotawa G (2005) Technical note: the Lagrangian particle dispersion model FLEXPART version 6.2. Atmos Chem Phys 5:2461–2474. https://doi.org/10.5194/acp-5-2461-2005

Tittlemier SA, Halldorson T, Stern GA, Tomy GT (2002) Vapor pressures, aqueous solubilities, and Henry's law constants of some brominated flame retardants. Environ Toxicol Chem 21:1804–1810

Ugranli T et al (2016) POPs in a major conurbation in Turkey: ambient air concentrations, seasonal variation, inhalation and dermal exposure, and associated carcinogenic risks. Environ Sci Pollut Res 23:22500–22512. https://doi.org/10.1007/s11356-016-7350-5

UNEP/POPS/COP.4/17 Recommendations of the persistent organic pollutants review committee of the Stockholm convention to amend annexes A, B or C of the convention. In: Stockholm Convention on Persistent Organic Pollutants, Stockholm, 4/2/2009 2009

Wang C et al (2012) Summer atmospheric polybrominated diphenyl ethers in urban and rural areas of northern China. Environ Pollut 171:234–240. https://doi.org/10.1016/j.envpol.2012.07.041

Wang Z-Y, Zeng X-L, Zhai Z-C (2008) Prediction of supercooled liquid vapor pressures and n-octanol/air partition coefficients for polybrominated diphenyl ethers by means of molecular descriptors from DFT method. Sci Total Environ 389:296–305. https://doi.org/10.1016/j.scitotenv.2007.08.023

Wania F, Dugani CB (2003) Assessing the long-range transport potential of polybrominated diphenyl ethers: a comparison of four multimedia models. Environ Toxicol Chem 22:1252–1261. https://doi.org/10.1002/etc.5620220610

Xiao H et al (2012) Atmospheric concentrations of halogenated flame retardants at two remote locations: the Canadian High Arctic and the Tibetan Plateau. Environ Pollut 161:154–161. https://doi.org/10.1016/j.envpol.2011.09.041

Xu H-Y, Zou J-W, Yu Q-S, Wang Y-H, Zhang J-Y, Jin H-X (2007) QSPR/QSAR models for prediction of the physicochemical properties and biological activity of polybrominated diphenyl ethers. Chemosphere 66:1998–2010. https://doi.org/10.1016/j.chemosphere.2006.07.072

Yang M et al (2013) Polybrominated diphenyl ethers in air across China: levels, compositions, and gas-particle partitioning. Environ Sci Technol 47:8978–8984. https://doi.org/10.1021/es4022409

Zhang B-Z, Zhang K, Li S-M, Wong CS, Zeng EY (2012) Size-dependent dry deposition of airborne polybrominated diphenyl ethers in urban Guangzhou, China. Environ Sci Technol 46:7207–7214. https://doi.org/10.1021/es300944a

Zhou S, Lee AKY, McWhinney RD, Abbatt JPD (2012) Burial effects of organic coatings on the heterogeneous reactivity of particle-borne benzo[a]pyrene (BaP) toward ozone. J Phys Chem A 116:7050–7056. https://doi.org/10.1021/jp3030705

Zhou S, Shiraiwa M, McWhinney RD, Poschl U, JPD A (2013) Kinetic limitations in gas-particle reactions arising from slow diffusion in secondary organic aerosol. Faraday Discuss 165:391–406. https://doi.org/10.1039/C3FD00030C